View metadata, citation and similar papers at core.ac.uk

brought to you by CORE

provided by UPCommons. Portal del coneixement obert de la UPC

UNIVERSITAT POLITÈCNICA DE CATALUNYA BARCELONATECH

UPCommons

Portal del coneixement obert de la UPC

http://upcommons.upc.edu/e-prints

Aquesta és una còpia de la versió *author's final draft* d'un article publicat a la revista *Mechanical Systems and Signal Processing*.

URL d'aquest document a UPCommons E-prints:

http://upcommons.upc.edu/handle/2117/104017

Article publicat / *Published paper*:

Pujol, G. et al. A velocity based active vibration control of hysteretic systems. "Mechanical Systems and Signal Processing", January 2011, vol. 25, Issue 1, p. 465-474. DOI: 10.1016/j.ymssp.2010.08.011

© 2017. Aquesta versió està disponible sota la llicència CC-BY-NCND 3.0 http://creativecommons.org/licenses/by-nc-nd/3.0/es/

A Velocity Based Active Vibration Control of Hysteretic Systems

Gisela Pujol[a,*], Leonardo Acho[a], Francesc Pozo[a], Arturo Rodríguez[b], Yolanda Vidal[a]

[a] *Departament de Matemàtica Aplicada III, Control Dynamics and Applications (CoDAlab), Universitat Politècnica de Catalunya, Escola Universitària d'Enginyeria Tècnica Industrial de Barcelona, Comte d'Urgell 187, E-08036 Barcelona, Spain*
[b] *Structural Department, Alstom-Power Wind, Ecotecnia Energías Renovables S.L., Roc Boronat, 78, E-08005 Barcelona, Spain*

Abstract

Hysteresis is a property of systems that do not instantly follow the forces applied to them, but react slowly, or do not return completely to their original state. A velocity based active vibration control, along with a special class of hysteretic models using passive functions are presented in this paper. This hysteretic model is based on a modification of the Bouc–Wen model, where a nonlinear term is replaced by a passive function. The proposed class retains the rate-independence property of the original Bouc–Wen model, and it is able to reproduce several kinds of hysteretic loops that cannot be reproduced with the original Bouc–Wen model. Using this class of hysteretic models, a chattering velocity-based active vibration control scheme is developed to mitigate seismic perturbations on hysteretic base-isolated structures. Our hysteretic model is used because of its simplicity in proving the stability of the closed-loop system; i.e., a controller is designed using the proposed model, and its performance is tested on the original hysteretic system, modeled with Bouc-Wen. Numerical experiments show the robustness and efficiency of the proposed control algorithm.

Keywords: Hysteresis, modeling, vibration control, passive function.

1. Introduction

The physical property called hysteresis can be defined as a memory-dependent (and also path-dependent) relation between excitation and response. It is a natural phenomenon encountered in a wide variety of processes like biology, optics, electronics, ferroelectricity, magnetism, mechanics, and structural systems, among other areas [1, 2]. On structural systems, hysteresis appears as a natural reaction of materials used to supply restoring forces against movements to dissipate energy [3]. Models of hysteresis have been reported, for instance, in [4, 5, 6, 7, 8]. Within the fields of civil and mechanical engineering, the Bouc–Wen model has been extensively employed to describe the hysteresis behavior of these systems [1, 3]. However, this dynamic model is quite complex as it has seven unknown parameters, which are not completely linearizable; this could represent a problem in the control design. Despite the versatility of the Bouc–Wen model in describing several hysteresis loops, this model cannot describe, for instance, asymmetric loops [9, 6], the tendency of change of hysteretic loops [10], pinching-like behavior, initial residual strain [11], or the Stribeck effect [12]. Based on Bouc-Wen model, we present a generalization of it that captures these behaviors, not losing the Bouc-Wen model properties. On the other hand, for the purpose of maintaining the seismic response of structures within safety, service and comfort limits, the combination of base isolators and feedback controllers (applying forces to the base) has been proposed in recent years. Active control, in front of passive or semi-active strategies, has the advantage of adaption to a wide range operating conditions and structures [13, 14, 15]

Two topics are developed in this paper. First, a class of hysteretic models using passive functions is presented. This class is based on a modification of the Bouc–Wen model, where the nonlinear term is replaced by a passive function.

*Corresponding author.
Email address: gisela.pujol@upc.edu (Gisela Pujol)
URL: http://www-ma3.upc.es/codalab/ (Gisela Pujol)

The proposed class maintains the rate-independence property [2] of the original Bouc–Wen model, and it is able to reproduce several kinds of hysteretic loops that cannot be reproduced with the original Bouc–Wen model. Furthermore, selecting appropriated parameters, our hysteretic model can accurately capture the hysteretic Bouc–Wen behavior. That is, different hysteretic behavior can be described by this model. Second, the problem of controlling hysteretic structural systems is addressed. The control objective is to design an active vibration controller that mitigates seismic disturbances on hysteretic base-isolated structures. Using velocity measurements, a chattering controller with a simple architecture for implementation is proposed. Lyapunov theory is invoked to validate the proposed controller, where we used the proposed hysteretic model because of its simplicity in proving the closed-loop stability. Moreover, numerical experiments applied to a base isolation system under the effect of seismic disturbances, where the original Bouc–Wen model is used to simulate the hysteretic behavior of the isolation, show the robustness and the efficiency of the proposed control algorithm. That is, we present a very simple and effective active control strategy that can be developed for actual hysteretic systems, adequately modeled by the proposed hysteretic model.

This paper is structured as follows. The proposed class of hysteretic models based on passive functions is presented in Section 2. Some particular cases, illustrating a set of hysteretic loops and its relation with some hysteretic loops observed experimentally, are presented. Moreover, numerical validation of the congruence of our model compared with the Bouc–Wen model is showed. In Section 3, a chattering controller is designed, based on velocity measurements only. Section 4 presents numerical simulations of a controlled base-isolated structure to give an overview of the controller's robustness. Finally, our conclusions are drawn in Section 5.

2. A class of passive hysteretic models

In this section, a class of hysteretic models is studied using a second-order structural hysteretic system given by [3] (pag. 24) and [16]:

$$m\ddot{x}(t) + c\dot{x}(t) + \Phi(x,t) = f(t) + u(t), \tag{1}$$

$$\Phi(x,t) = \alpha k x(t) + (1-\alpha)Dkz(t), \tag{2}$$

$$\dot{z}(t) = D^{-1}(A\dot{x}(t) - \beta|\dot{x}(t)||z(t)|^{n-1}z(t) - \lambda\dot{x}(t)|z(t)|^{n}), \tag{3}$$

where m and c are the mass and the damping coefficients, respectively; Φ represents the nonlinear restoring force; x gives the base displacement position (relative position with respect to foundation); $f(t) = -m\ddot{x}_g$ is the excitation force, where $\ddot{x}_g$ is the earthquake ground acceleration and $u(t)$ is the (active) control input. Note that an upper bound exists for the seismic perturbation, that is, there exists an unknown positive constant F such that:

$$|f(t)| \leq F \quad \text{for all} \quad t \geq 0. \tag{4}$$

Equations (2)-(3) represent the restoring force $\Phi(x,t)$ by superposing an elastic component αkx and a hysteretic component $(1-\alpha)Dkz$, in which $D > 0$ is the yield constant displacement and $\alpha \in (0,1)$ is the post- to pre-yield stiffness ratio; A, β, n and λ are the non-dimensional Bouc–Wen model parameters. We set $\beta - \lambda > 0$, which corresponds to a special case of physical hysteretic behavior [3]. These parameters control the shape and size of the hysteresis loop [17]. So, the Bouc-Wen model parameters are $\alpha, k, D, A, \beta, n$ and λ. The variable $z(t)$ is an internal state which is not accessible for measurements. The schematic representation of the system (1)-(3) is given in Figure 1.
To deduce a class of hysteretic models using passive functions, the nonlinear terms in (3) are replaced by a family of passive functions as follows:

$$\dot{z}(t) = G(\dot{x}, g(z)) = D^{-1}\Big(A\dot{x}(t) - g(z(t))\,|\dot{x}(t)|\Big), \tag{5}$$

where the function $g(z)$ is a passive function satisfying

$$z(t)\cdot g(z(t)) \geq 0 \quad \text{and} \quad g(0) = 0 \quad \text{for all} \quad t \geq 0. \tag{6}$$

Proposition 1. *The dynamic system $\dot{z}(t) = G(\dot{x}, g(z)))$ in equation (5) is rate-independent, with G continuos.*

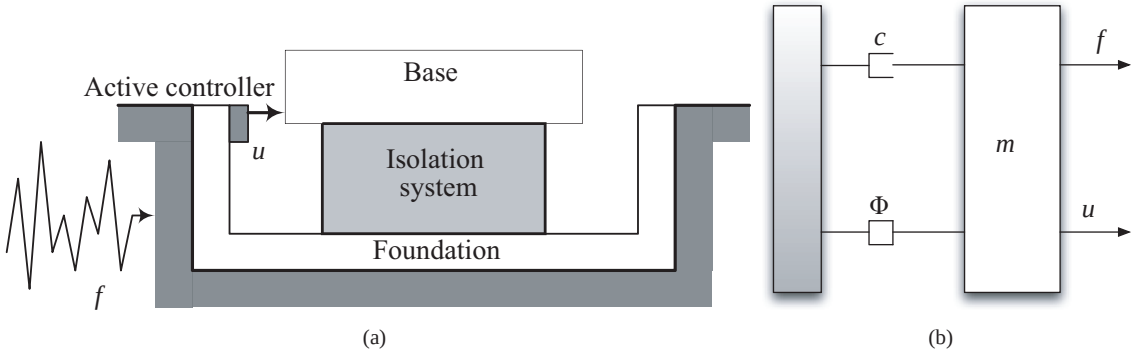

Figure 1: (a) Base isolation system and (b) schematic model of structural hysteretic system (1)-(3).

Proof.- The system (5) is a special case of the Duhem model, and therefor it is rate-independent [2, 18]. Note that the passivity property of the function $g(z(t))$ gives a sufficient, but not necessary, condition for the rate-independence. Let's see it. Consider $\tau(t)$ be a positive time-scale (see [19]). Then $\tau(0) = 0$ and, thus, $z_\tau(0) = z(\tau(0)) = z(0) = z_0$. Now, for all $t > 0$, consider

$$\frac{dz_\tau(t)}{dt} = D^{-1}\left(A\frac{dx_\tau(t)}{dt} - g(z_\tau(t))\left|\frac{dx_\tau(t)}{dt}\right|\right)$$
$$\dot\tau\frac{dz(\tau)}{d\tau} = D^{-1}\left(A\dot\tau\frac{dx(\tau)}{d\tau} - g(z(\tau))\left|\dot\tau\frac{dx(\tau)}{d\tau}\right|\right).$$

Since τ is a positive time scale, $\dot\tau(t) \geq 0$. Hence, it follows that:

$$\dot\tau\frac{dz(\tau)}{d\tau} = D^{-1}\left(A\dot\tau\frac{dx(\tau)}{d\tau} - \dot\tau g(z(\tau))\left|\frac{dx(\tau)}{d\tau}\right|\right)$$
$$\frac{dz(\tau)}{d\tau} = D^{-1}\left(A\frac{dx(\tau)}{d\tau} - g(z(\tau))\left|\frac{dx(\tau)}{d\tau}\right|\right),$$

as required. □

Remark 1.- Function $G(\dot x, g(z)))$ is positively homogeneous with respect to $\dot x$; that is $D^{-1}(A\alpha\dot x - g(z)|\alpha\dot x|) = \alpha D^{-1}(A\dot x - g(z)|\dot x|)$.

To illustrate a set of hysteretic loops that can be captured by the proposed model in equation (5), we carry out a few simulations. For this purpose, consider the system (1)-(2) with $m = 1$ kg, $c = 0$ Ns/m, $k = 1$ N/m, $D = 1$ m, $f(t) = 0$ N, $\alpha = 0$, $A = 1$, and $u(t) = \sin((0.03t + 0.2)t)$ [17]. The following cases are studied (hereafter we omit to specify time dependency to simplify writing):

Case 1: $g(z) = Az$,

Case 2: $g(z) = \tanh(z)$,

Case 3: $g(z) = \begin{cases} \sin(1.5z)\,, & |z| < 0.5 \\ 0.5z^3\,, & \text{otherwise} \end{cases}$,

Case 4: $g(z) = \begin{cases} \sin(0.75)\,, & z \geq 0.5 \\ \sin(1.5z)\,, & z \in (0\,,\, 0.5) \\ z\,, & z \in (-0.5\,,\, 0] \\ 0.5\,z^3\,, & \text{otherwise} \end{cases}$,

Case 5: $g(z) = \rho_0 \operatorname{sech}(\frac{z}{a}) \cdot \tanh(\frac{z}{a})$, where $\rho_0 = 1$ and $a = 1$.

Using Case 1 and 2, asymmetric hysteretic loops (with respect to the origin) are seen in Figure 2, this behavior can also be offered in [17]. This hysteretic behavior may be attributed to materials that have an *initial residual strain*, like a building structural frame. This initial residual deformation, which will be permanent and progressive with time, is due to the multiple cycles (low and high frequency) along the structure life, attributed to earthquakes, wind loading, ultimate loads, service loads, structural degradation, among many others. A subsequent peak of an earthquake acceleration will catalyze a further displacement of the structure from its origin. In Case 3, shown in Figure 3, the asymmetric loops resemble a pinching-like behavior in the main loop, as observed in [11]. This may be attributed to reinforced concrete structures where this type of behavior is common under dynamic loads. Case 4 (Figure 3) shows a type of behavior often seen in electrical substations [9]. Finally, in Case 5 (Figure 4), the passive function $g(z)$ captures the Stribeck effect as in [20] and [21]. The above hysteretic loops cannot be reproduced with the original Bouc–Wen model.

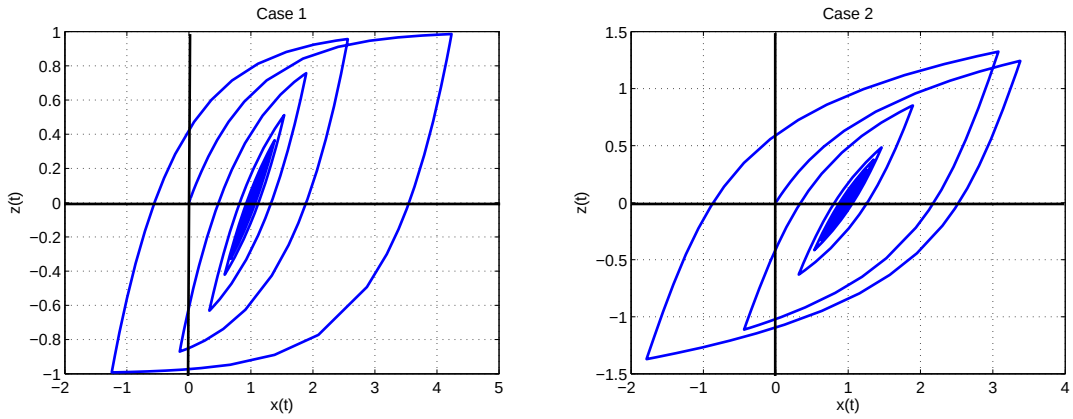

Figure 2: Hysteretic loops for Cases 1 and 2.

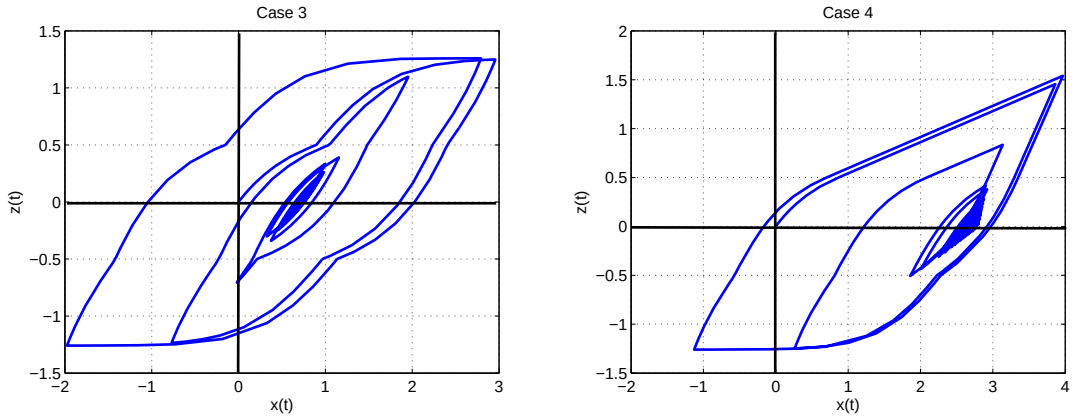

Figure 3: Hysteretic loops for Cases 3 and 4.

To complete this section a comparison with the Bouc–Wen model is presented. Let the system (5) be as follows:

$$\dot{z} = D^{-1}(A\dot{x} - (a_1 z + a_2 z^2 + a_3 z^3)|\dot{x}|), \tag{7}$$

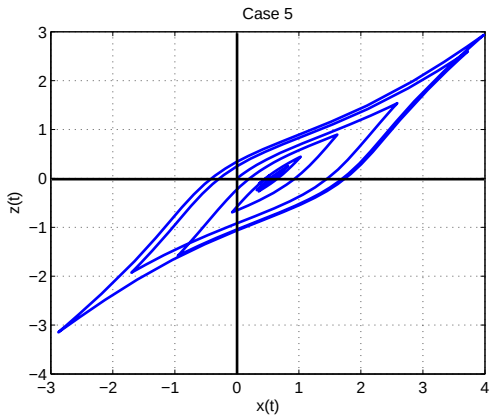

Figure 4: Hysteretic loops for Case 5.

that is, $g(z) = a_1 z + a_2 z^2 + a_3 z^3$ in equation (5). First, we consider the Bouc–Wen dynamic (3) with the following nominal values: $D = 1$ m, $A = 1.2$, $\beta = 3$, $\lambda = 3$ and $n = 1.1$, as in [3]. For the proposed model (7), we take $D = 1$ m, $A = 0.9$, $a_1 = 4.15$, $a_2 = 0$, and $a_3 = 0.6$. Both models, (7) and (3), have $\dot{x}(t)$ as their input signal. Selecting $\dot{x}(t) = \sin(t) + \sin(3t) + \sin(7t) + \sin(9t)$ the simulation results of the system response ($z(t)$) are shown in Figure 5. This figure shows that it is feasible to find a passive function $g(z)$ such that the system (5) can reproduce the Bouc–Wen hysteresis behavior.

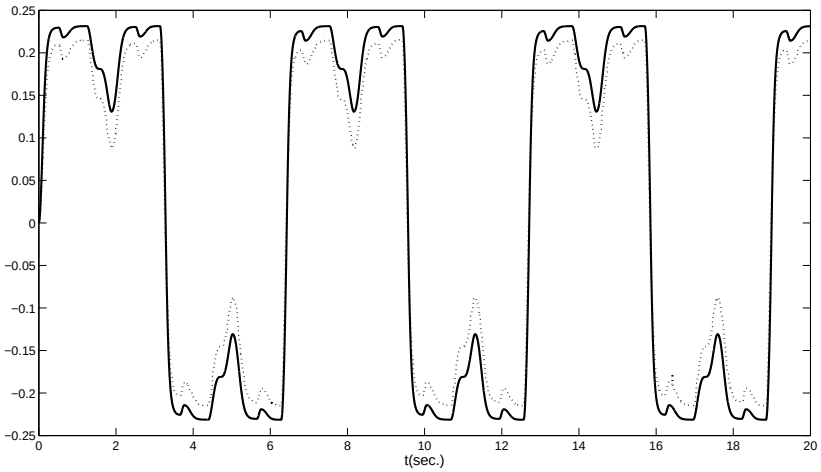

Figure 5: A Comparison between the proposed (dotted-line) and the Bouc–Wen (solid line) models.

The passivity of the function introduced in equation (5) makes this model appropriate for control design. This control design is then presented in the next section.

3. Control design

The control objective is to design a static controller that reduces the vibrations produced by the seismic disturbance by using only velocity measurements. The next theorem states the main contribution with respect to the control design.

Theorem 1 *The system in equations (1), (2) and (5) defines a bounded-input bounded-output (BIBO) stable system with:*

$$u = -\rho \operatorname{sgn}(\dot{x}) \,, \tag{8}$$

where ρ is a positive constant design parameter. Moreover, when $\rho \geq F$ where F is given by (4), a Lyapunov-stable system is obtained and the controller (8) *mitigates the seismic disturbance.*

Proof.- Given the Lyapunov function

$$V(x, \dot{x}, z) = \frac{\alpha k}{2m} x^2 + \frac{1}{2}\dot{x}^2 + \frac{(1-\alpha)D^2 k}{2mA} z^2, \tag{9}$$

as an energy expression, the time derivative along the system in equations (1), (2) and (5) yields

$$\begin{aligned}
\dot{V} =& \frac{\alpha k}{m} x\dot{x} + \dot{x}\ddot{x} + \frac{(1-\alpha)D^2 k}{mA} z\dot{z} \\
=& \frac{1}{m}\left(\dot{x}\left[m\ddot{x} + \alpha k x\right] + \frac{(1-\alpha)D^2 k}{A} z\dot{z}\right) \\
=& \frac{1}{m}\left(\dot{x}\left[-c\dot{x} - (1-\alpha)Dkz + f(t) - \rho \operatorname{sgn}(\dot{x})\right] + \frac{(1-\alpha)D^2 k}{A} z\dot{z}\right) \\
=& \frac{1}{m}\left(-c\dot{x}^2 - (1-\alpha)Dkz\dot{x} + f(t)\dot{x} - \rho \operatorname{sgn}(\dot{x})\dot{x} + \frac{(1-\alpha)D^2 k}{A} z\left[\frac{1}{D}A\dot{x} - \frac{1}{D}g(z)|\dot{x}|\right]\right) \\
=& \frac{1}{m}\left(-c\dot{x}^2 + f(t)\dot{x} - \rho|\dot{x}| - \frac{(1-\alpha)Dk}{A} z g(z)|\dot{x}|\right)
\end{aligned}$$

$$\leq \frac{1}{m}\left(-c\dot{x}^2 - \underbrace{(\rho - |f(t)|)}_{\geq 0}|\dot{x}| - \frac{(1-\alpha)Dk}{A}\underbrace{z g(z)}_{\geq 0}|\dot{x}|\right) \leq \frac{1}{m}\left(-c\dot{x}^2 - (\rho - F)|\dot{x}|\right).$$

When $\rho \geq F$, since $g(z)$ is a passive function, we obtain $\dot{V} \leq 0$, implying that the closed-loop system (1), (2), (5) and (8) is stable in the Lyapunov sense. To demonstrate the seismic attenuation, let us compare the Lyapunov time derivatives of the open-loop and closed-loop systems, i.e., $\dot{V}_{OL}$ and $\dot{V}_{CL}$. From (9),

$$\dot{V}_{CL} = \dot{V}_{OL} - \frac{1}{m}\rho|\dot{x}| \Rightarrow \dot{V}_{CL} < \dot{V}_{OL}. \tag{10}$$

Next we define the transient decay rate for both cases as in [20]:

$$\zeta = \frac{-\dot{V}(x)}{V(x)}.$$

From (10), we deduce that

$$\zeta_{CL} > \zeta_{OL}.$$

We conclude that the closed-loop system has a larger transient decay rate response than the uncontrolled system, thus mitigating the seismic disturbance.

When $\rho < F$, it has been obtained that

$$\dot{V} \leq \frac{1}{m}\left(-c\dot{x}^2 - (\rho - F)|\dot{x}|\right),$$

which can be rewritten as

$$\dot{V} \leq -\frac{1}{m}\left(c|\dot{x}| - (F - \rho)\right)|\dot{x}|.$$

Thus, when $|\dot{x}| \geq \frac{F-\rho}{c}$ then $\dot{V} \leq 0$, implying that the closed-loop system (1), (2), (5) and (8) remains bounded. □

Remark 2.- *Note that if accelerometers are employed instead of velocity sensors, velocity information can still be extracted [22]. In fact, only the sign of the velocity, quantity that can be achieved implicitly, is required (peaks at displacement signal).*

Remark 3.- *The signum function in the control law in Theorem 1, which is commonly used in sliding mode control theory, produces chattering [23]. One way to avoid chattering is to replace the signum function by a smooth sigmoid-like function such as*

$$\nu_\delta(\dot{x}(t)) = \frac{\dot{x}(t)}{|\dot{x}(t)| + \delta}, \tag{11}$$

where δ is a sufficiently small positive scalar.

Remark 4.- *For control implementation, the gain ρ satisfying the condition of Theorem 1 may be too large for an actuator to provide. In this case, the controller performance is evaluated using some realistic value of this gain. This is the objective of the following sections.*

Remark 5.- *It has been also proven [22] that the proposed controller also stabilizes the system under the Bouc–Wen model.*

4. Simulation and experimental proposal

In this section, a numerical example is presented to demonstrate the effectiveness of the proposed controller defined in Theorem 1. We test the robustness of the control scheme (11) when it is applied to a more complex realistic structure: a hysteretic, base-isolated, eight-story building that is similar to existing buildings in Los Angeles (California) [24]. As said in section 2, selecting appropriated parameters of the proposed hysteric model (5), it can capture the hysteretic Bouc-Wen behavior. So, despite the numerical simulation are done using the original hysteretic Bouc-Wen model, the stability is preserved.

We set $\delta = 0.05$ in (11) and $\rho = 5.05 m_0$ N in (8), where $m_0 = 3565.7 \times 10^3$ is the building base mass. With this controller gain, the maximum controller force is about 50% of the total building mass (see Table 1). The evaluation is reported in terms of two performance indices: Q_1, defined as the peak base displacement in the controlled structure normalized by the corresponding displacement in the uncontrolled structure, and Q_2, is the peak absolute floor acceleration in the controlled structure normalized by the corresponding acceleration in the uncontrolled structure. The controlled structure – whose parameters are described in Tables 1-2 – is simulated for seven earthquake ground accelerations (Newhall, Sylmar, El Centro, Rinaldi, Kobe, Ji-Ji and Erzinkan) and Table 3 presents the values of indices Q_1 and Q_2 under these earthquakes. All the excitations are used at their full intensity for the evaluation of the performance indices. Performance indices larger than 1 indicate that the response of the controlled structure is larger than that of the uncontrolled structure. These quantities are highlighted in bold. In this paper, the controllers are assumed to be fully active. These actuators are used to apply the active control forces to the base of the structure. In this control strategy, almost all the response quantities are substantially reduced from the uncontrolled cases. More precisely, the reduction in base displacement is around 90% in all cases, and the floor accelerations are also reduced by 38-75% in a majority of earthquakes (except El Centro). For the El Centro case, where $Q_2 = 1.3292$, this value is above one. This could be because of the earthquake behavior , such as: frequency contents, time duration, dynamic range, DC-component, etc. However, this value can be improved if we increase the controller gain.

The benefit of this active control strategy is the reduction of base displacements (Q_1) without increasing the acceleration (Q_2). The reduction of the peak base displacement Q_1 of the base-isolated building is one of the most important criteria during strong earthquakes. At the same time, reducing acceleration levels is crucial for non-structural components, which account for 75% of the damage during an earthquake.

For the base-isolated buildings, superstructure drifts are reduced significantly compared to the corresponding fixed buildings because of the isolation from the ground motion. Hence, a controller that reduces or does not increase the peak superstructure, while reducing the base displacement significantly, is desirable for practical applications [25]. In this respect, the proposed active controller performs well.

4.1. Time-history plots

Figures 6-8 show the time-history plots of various response quantities for the uncontrolled building and the building with active controllers using one of the seven earthquakes. More precisely, Figure 6 presents the plots for the base displacement under Erzinkan for both the uncontrolled and the controlled scenarios. The quantities plotted in Figure 7 are the absolute acceleration of the base for the uncontrolled and controlled situations. The magnitude of the control signal in Figure 8[1] seems reasonable in comparison to the seismic excitation acceleration $a(t)$ plotted in Figure 9.

Table 1: Model coefficients of the hysteretic base-isolated eight-story building.

	mass ($\times$1000 kg)	**stiffness** (N/m)	**damping** (Ns/m)
base	3565.7	919422	101439
1st floor	2580	12913000	11363
2nd floor	2247	10431000	10213
3rd floor	2057	7928600	8904
4th floor	2051	5743900	7578
5th floor	2051	3292800	5738
6th floor	2051	1674400	4092
7th floor	2051	496420	2228
8th floor	2051	496420	704

Table 2: Parameters of the hysteresis model in Equations (2)-(3)

$\alpha = 0.5$	$A = 1$
$k = 6466100$ N/m	$\beta = 0.5$
$D = 0.0245$ m	$\lambda = 0.5$
$n = 1$	

Table 3: Performance indices obtained by the numerical simulations.

	Q_1	Q_2
Newhall	0.0750	0.6211
Sylmar	0.0355	0.4051
El Centro	0.1032	**1.3295**
Rinaldi	0.0643	0.4570
Kobe	0.1158	0.4051
Ji-Ji	0.1165	0.4830
Erzinkan	0.0633	0.2530

[1]This control signal is not of the *signum* display because we are employing its smooth version (see Remark 1).

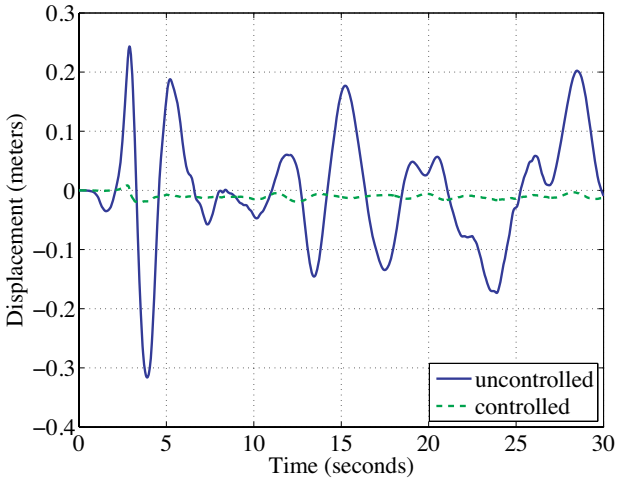

Figure 6: Time-history response under Erzinkan excitation. Closed-loop displacement (dashed) and open-loop displacement (solid).

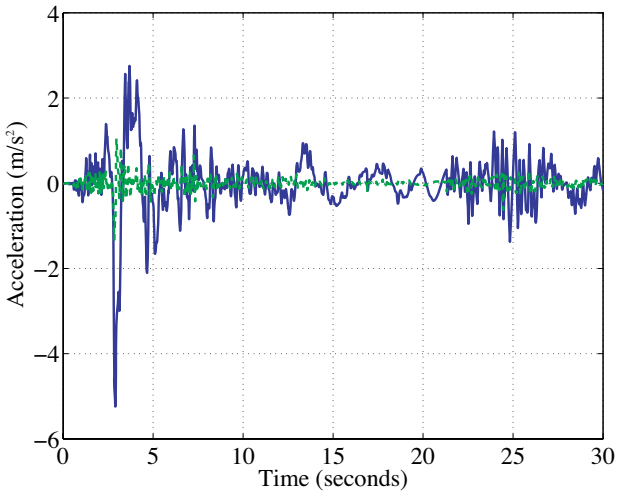

Figure 7: Time-history response under Erzinkan excitation. Closed-loop acceleration (dashed) and open-loop acceleration (solid).

Looking at Figure 6, it is clear that the controlled relative displacement of the base is significantly reduced compared to the uncontrolled case. Figure 7 shows that the reduction in the absolute base acceleration is not as drastic but is still significant.

5. Conclusions

A class of passive Bouc–Wen models has been presented in this paper where a nonlinear term of the original Bouc–Wen model has been replaced by a passive function. The proposed class maintains rate-independence property and reproduces hysteretic loops that have been previously observed. Furthermore, selecting appropriated parameters, this class of hysteretic model can capture the Bouc-Wen model behavior. Using the proposed hysteretic model representations due to its simplicity, a control scheme using only velocity measurements has been developed. The robustness of the controller is tested using the original Bouc–Wen model through numerical simulations. The controller's performance has been validated with numerical experiments in a more realistic base-isolated building structure.

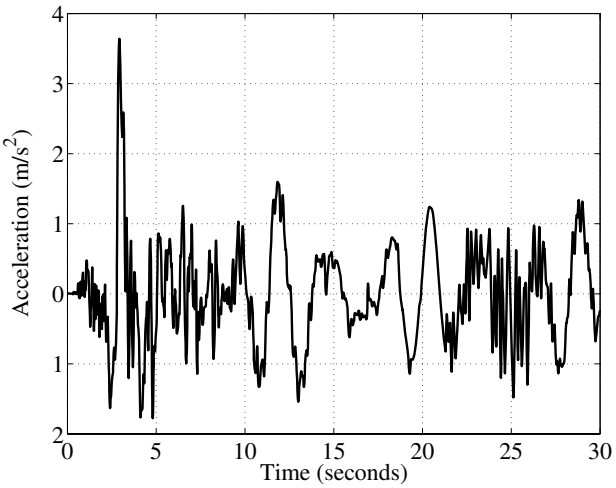

Figure 8: Control signal (acceleration $u(t)/m$).

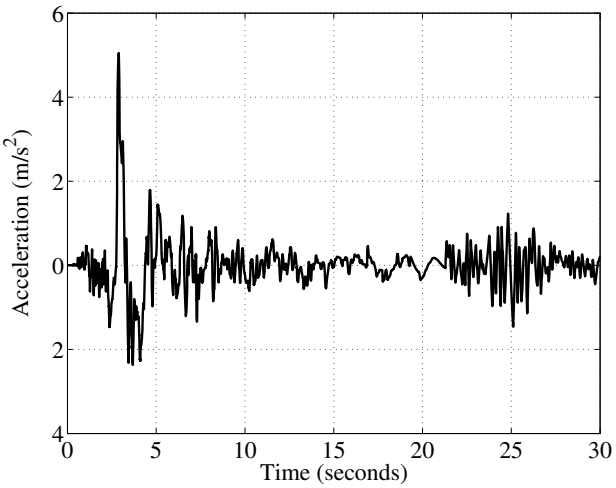

Figure 9: Erzinkan earthquake ground acceleration.

Acknowledgements

This work was supported by CICYT through grant DPI2008-06463-C02-01. Also, the authors would like to acknowledge the reviewers comments.

References

[1] M. Ismail, F. Ikhouane, J. Rodellar, The Hysteresis Bouc–Wen Model, a Survey, Arch. Comput. Methods Eng. 16 (2009) 161-188.
[2] J. Oh, S. Bernstein, Semilinear Duhem Model for Rate-Independent and Rate-Dependent Hysteresis, IEEE Tran. on Aut. Ctrol. 50(5) (2005) 631-645.
[3] F. Ikhouane, J. Rodellar, Systems with Hysteresis: Analysis, Identification and Control Using the Bouc–Wen Model (pag. 24, 165), John Wiley and Sons, Ltd., England (2007).
[4] L. Chua, C. Steven, A Generalized Hysteresis Model, IEEE Tran. on Circuit Theory 19(1) (1972) 36-48.
[5] R.P. Clarke, Non-Bouc Degrading Hysteresis Model for Nonlinear Dynamic Procedure Seismic Design, Journal of Structural Eng. 31(2)(2005) 287-291.

[6] J. Song, A. Kiureghian, Generalized Bouc–Wen Model for Highly Asymmetric Hysteresis, Journal of Eng. Mechanics 132(6)(2006) 610-618.
[7] G. Bertotti, I. Mayergoyz, The Science of Hysteresis, Elsevier Inc (3-Volume set), UK (2005)
[8] F. Pozo, L. Acho, A. Rodríguez, G. Pujol, Nonlinear Modeling of Hysteretic Systems with Double Hysteretic loops Using Position and Acceleration Information, Nonlinear Dynamics 57(1-2) (2009) 1-12.
[9] A. Filiatrault, S. Kremmidas, A. Elgamal, F. Seible, Substation Equipment Interaction-Rigid and Flexible Conductor Studies, Rep. No. SSRP-99/00, University of California, San Diego, California, (1999).
[10] Y.Z. Wu, D.L. Yao, Z.Y. Li, Hysteresis Loop of a Ferroelectric Bilayer with an Antiferroelectric Interfacial Coupling, Journal of Applied Physics 91(3) (2002) 1482-1486.
[11] N. Mostaghel, Analytical Description of Pinching, Degrading Hysteretic Systems, Journal of Eng. Mechanics 125(2) (1999) 216-224.
[12] F. Auricchio, L. Faravelli, G. Magonette, V. Torra, Shape Memory Alloys: Advances in Modeling and Applications, CIMNE, Barcelona, Spain (2001).
[13] A. Baratta, O. Corbi, Dynamic response and control of hysteretic structures, Simulation Modelling Practice and Theory 11(5-6) (2003) 371-385.
[14] B. F. Spencer Jr., S. Nagarajaiah, State of the Art of Structural Control, Journal of Structural Engineering 129(7) (2003) 845-856.
[15] F. Pozo, F. Ikhouane, G. Pujol, J. Rodellar, Adaptive backstepping control of hysteretic base-isolated structures, Journal of Vibration and Control 12(4) (2006), 373? 394.
[16] F. Ikhouane, V. Manosa, J. Rodellar, Adaptive control of a hysteretic structural system, Automatica.
[17] A.W. Smyth, S.F. Masri, E.B. Kosmatopoulos, A.G. Chassiakos, T.M. Caughey, Development of adaptive modeling techniques for non-linear hysteretic systems, International Journal of Non-Linear Mechanics 37(8) (2002) 1435-1451.
[18] K. Ashwani, D. Bojona, O. Jinhyoung, D. Rizos, D. Spilios, S. Bernstein, Duhem Modeling of Friction-Induced Hysteresis, IEEE Control Systems Magazine (2008) 90-107.
[19] Oh J.H., and Bernstein S., "Semilinear Duhem model for rate-independent and rate-dependent hysteresis", *IEEE Transactions on Automatic Control*, **50**(5), 631–645, 2005.
[20] J.S. Liu, S.L. Chen, On Global Stability of Quadratic State Feedback Controlled Linear Systems, Systems and Control Letters 21 (1993) 371-379.
[21] K. Wilde, P. Gardoni, Y. Fujino, Base Isolation System With Shape Memory Alloy Device for Elevated Highway Bridges, Engineering Structures 22(3) (2000) 222-229.
[22] F. Pozo, P. Montserrat, J. Rodellar, L. Acho, Robust Active Control of Hysteretic Base-Isolated Structures: Application to the Benchmark Smart Base-Isolated Building, Structural Control and Health Monitoring 15(5) (2008) 720-736.
[23] C. Edwards, S.K. Spurgen, Sliding Mode Control. Theory and applications., pag. 24, Taylor and Francis Ltd., London, 1998.
[24] S. Narasimhan, S. Nagarajaiah, E.A. Johnson, H.P. Gavin, Smart Base-Isolated Benchmark Building. Part I: Problem Definition, Structural Control and Health Monitoring 13(2-3)(2006) 573-588.
[25] Z. Xu, A.K. Agrawal, J.N. Yang, Semi-Active and Passive Control of the Phase I Linear Base-Isolated Benchmark Building Model, Structural Control and Health Monitoring (13)(2-3)(2006) 626-648.